DELIVERABLE REPORT

Deliverable:	D5.3: QCM- and QCM-array platforms for in situ assessment of MNM-protein, -cell and receptor interactions
Work Package:	WP5: MNM interactions with biomolecules and environmental factors
Lead Beneficiary:	Attana AB
Nature of Deliverable:	Report
Dissemination Level:	Public (PU)
Delivery Date:	31/08/2015
Submitted By:	Diluka Peiris, Teodor Aastrup (Attana)
Revised By:	Carsten Weiss (KIT) and Douglas Gilliland (JRC)
Approved By:	Marco Monopoli (UCD) and Iseult Lynch (UoB)

Project full title: “Engineered nanomaterial mechanisms of interactions with living systems and the environment: a universal framework for safe nanotechnology"

Grant agreement no: NMP4-LA-2013-310451

Contents

1.0 Introduction

With the recent advances in nanotechnology and the rapid increase in use of manufactured nanomaterial (MNMs) in biomedical and biotechnical applications, their release into the environment has become a major concern. This necessitates understanding their fate and behaviour in living systems and in the environment. It is now well accepted that when MNMs come into contact with a complex biological media, e.g., blood after systemic administration, they rapidly get coated by a selected group of biomolecules (Monopoli *et al* 2012; Rahman *et al* 2013) forming the corona that acts as an interface between the MNM and the biological species. The MNM physiochemical properties are believed to be capable of influencing the protein (and other biomolecule) composition of the corona (Monopoli *et al* 2011, Nel *et al* 2009) and also the biological composition of the exposure environment can lead to specific interactions (as the nature of the corona reflects the biological media). While significant effort has been dedicated to revealing the biological identity of the MNM corona by means of proteomics techniques (Lundqvist *et al* 2011, Goppert *et al* 2005, Sakulkhu *et al* 2014, Tenzer *et al* 2013), the implementation of nanotechnologies both in medicine and other consumer products is currently hampered by the lack of understanding of the mechanism of MNM interaction with living systems and the mechanisms of interactions between MNM-corona and cellular receptors remain obscure.

The surface plasmon resonance technique has recently been utilised to investigate the binding of MNMs onto putative biological targets using target proteins immobilised onto sensor surfaces (Canovi et al, 2012). However, interactions between MNMs and the target proteins are yet to be studied in a more relevant biological environment.

For this purpose, Attana Quartz Crystal Microbalance (QCM) technology offers a highly adaptable means to investigate surface functionality in biological environments. It offers a label free, cost effective approach, whereby immobilised target layers can be assembled at sensor surfaces to investigate interactions of interest. NanoMILE task 5.3 was aimed at developing a platform for the characterisation of interactions between bio-nano interface (i.e. the layer of biomolecules adsorbed at the MNM surface) and its cell binding partners. This new biosensor system is based on the Attana QCM technology and utilised adherent cells directly grown on the surface of a

sensor or immobilised using biomolecules, in contrast to the conventional QCM biosensor system where the biological receptors are often the purified biomolecules. The Attana cell based QCM system has previously been successfully utilised to study molecular interactions on adherent and suspension cells (Elmlund et al, 2015, Peiris et al, 2012).

1.1 Quartz Crystal Microbalance (QCM) Technology

QCM is a label free technique for mass detection. It relies on the piezo-electric effect, the phenomenon that occurs when a crystal vibrates mechanically if exposed to an oscillating electric potential, and *vice versa*, whereby the crystal gives an electric signal if deformed.

The piezoelectric behaviour of quartz crystals is utilized in QCM biosensors as well as in devices such as watches, computers and televisions. Each crystal has its own resonance frequency, which is dependent on the mass or thickness of the crystal. Thinner crystals resonate at higher frequencies and are consequently more sensitive, however, a drawback is that the crystal become more fragile. The Attana QCM uses an AT-cut crystal (where the quartz is cut at an angle of 35^{o} 15' from the Z-axis, as shown in Figure 1) and the usual frequency region is around 10 MHz. When a molecule attaches to the crystal surface, the system becomes heavier and the resonance frequency decreases, creating a very sensitive microbalance.

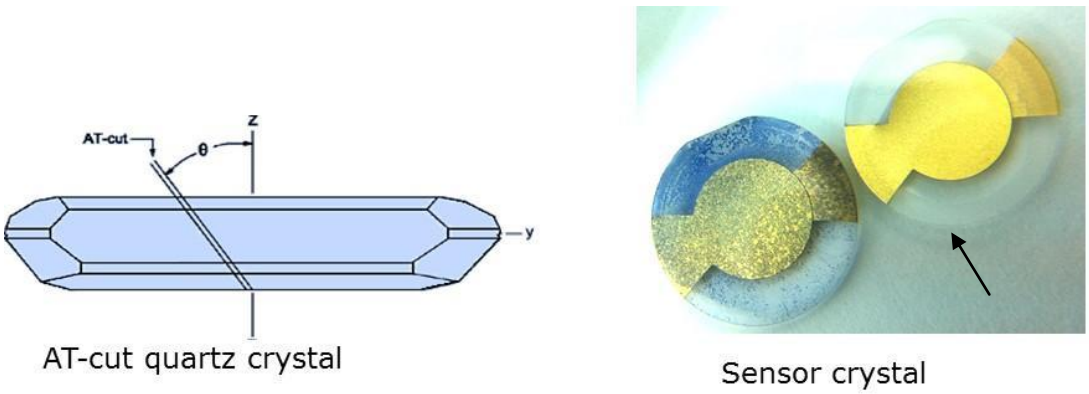

Figure 1: AT-cut quartz crystal (left) and quartz crystal sandwiched between gold electrodes (right)

Under certain constant conditions, the change of resonance frequency is linearly proportional to the mass change, as shown in Figure 2. The Sauerbrey equation (1959), which describes the relationship between the change in frequency and the change in adsorbed mass is given below:

$$\Delta m = \frac{-\Delta f A (\rho_q \mu_q)^{\frac{1}{2}}}{2 f_0^{\,2}}$$

where Δm (gcm^{-2}) is the adsorbed mass per unit area, Δf the frequency change, A the area of the gold surface (0.159 cm^2), f_0 the fundamental mode resonant frequency of the crystal (~10 MHz), p_q the density of quartz (2.648 gcm^{-3}) and μ_q the shear modulus of quartz (2.947x10^{11} gcm $^{-1}$ s $^{-2}$).

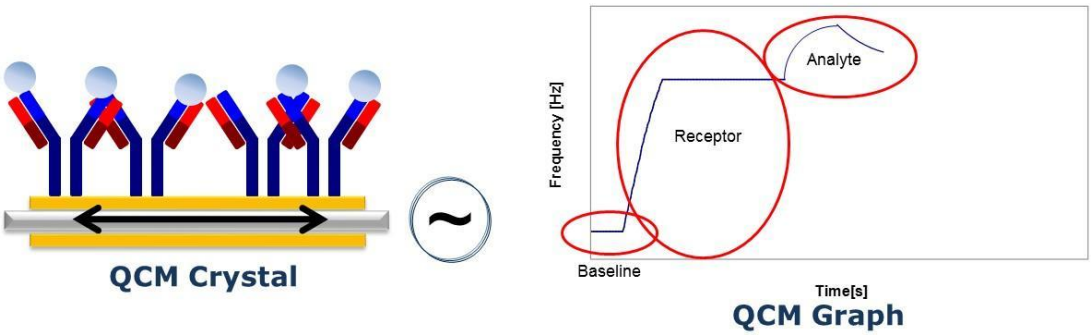

Figure 2: Changes of resonance frequency due to the increase of mass on the surface.

Results from real time QCM measurements on the Attana system can be presented as a sensogram which is a plot of frequency change against time (see example in Figure 2).

After the injection of the sample of interest, association with the surface is observed for a given amount of time, after which the system is switched back to having only running buffer flowing over the surface. During this step,dissociation of analyte from the surface is the only process occurring as no new analyte is available for binding. The rate of analyte binding to the antigen, k_a (association rate constant) and the rate of analyte detaching from the antigen k_d (dissociation rate constant) can be derived from the sensorgram, with the relevant equations shown in Figure 3.

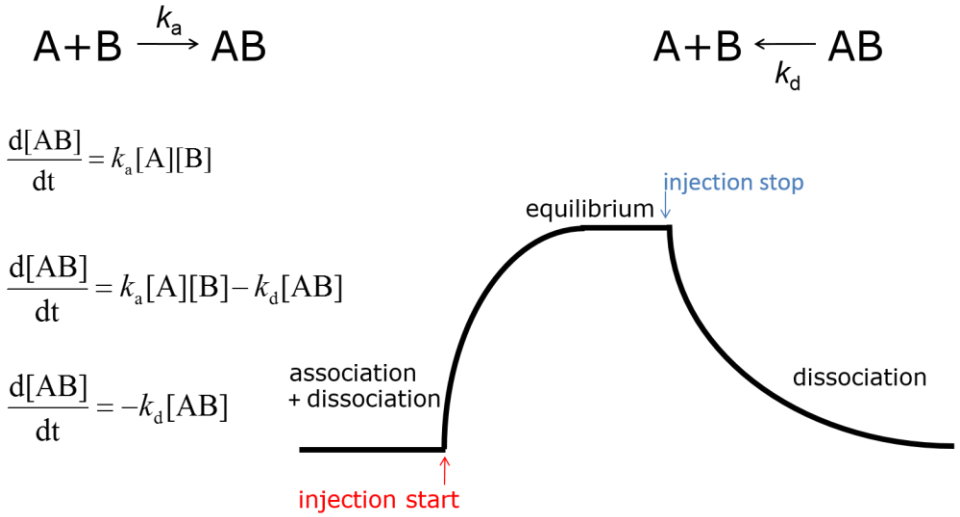

Figure 3: Sensorgram and rate constants

1.2 Attana Cell 200 system

The Attana Cell 200 system is a dual channel, label free, temperature controlled, continuous flow system for automated (Attana Cell A200) or manual (Attana Cell 200) analysis of molecular interactions (Figure 4). Attana Cell 200 facilitates both conventional biochemical assays and cell based assays allowing unattended analysis of up to 192 samples using pre-programmed methods.

Figure 4. Attana Cell 200 system

The key feature of the Attana Cell 200 is that it enables kinetic characterisation of interactions with cell surface targets, in real time using cells immobilised on a sensor surface. The all-in-one ability to cultivate, treat and analyse the cells directly on the sensor surface minimises handling and perfects cell conditioning. It is also possible to capture the cells directly from cell suspensions using cell surface binding antibodies or lectins. As the instrument is temperature controlled, chemically resistant and uses continuous flow, interactions can be studied at physiological conditions such as normal salinity, 37 ^{o}C and under various flow rates.

In D5.3, which reports on the activities undertaken within NanoMILE WP5 Task 5.3, Attana has used a newly developed platform whereby cells have been grown directly on the chip surface, thereby providing a more biologically relevant system to enable detailed studies of cell-ligand interactions (Figure 5). This new system allows quantitative evaluation of molecular interactions in a much more relevant cellular environment compared with conventional systems which utilise immobilised proteins (as example receptors) on the sensor surface.

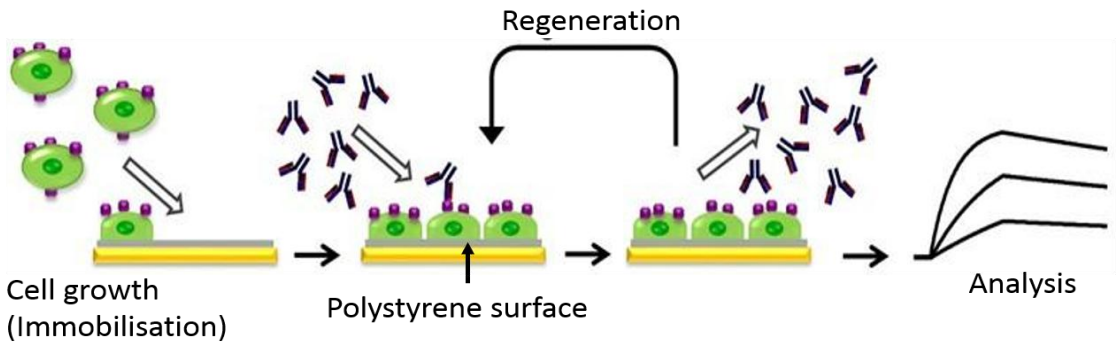

Figure 5: Graphic representation of a cell based experimental layout using the Attana Cell 200 QCM.

The chip holds a polystyrene sensor on the surface that optimises the cell growth on it (COP-1 surfaces) with the particular advantages that the cells can grow on the surface without further surface modification (Figure 6). Quite interestingly, more than 30 human cell lines have been successfully grown on these polystyrene surfaces, including, for example, human colon adenocarcinoma cells (KM-12) and ovary adenocarcinoma cells (SKOV-3) (Li et al., 2015), human breast cancer *cells* (MCF-7) (Yazdan Madani et al., 2012), and human acute lymphocytic leukemia cells (Jurkat) (Li et al., 2013).

Figure 6: Attana COP-1 chip with chamber for cell culture medium.

2.0 METHOD DEVELOPMENT

The binding of analytes to cell surfaces can be monitored in real time by passing analytes over adherent cells, however to fully evaluate the use of the Attana cell 200 system for assessment of MNM interactions with cells, it is of utmost importance to identify the different parameters and experimental settings that can lead to false positive results and to experimental variability.

For example the molecular interactions on cellular surfaces is based on several parameters including the cell line, cell seeding density, buffer conditions, biofluids used and temperature. Cellular surfaces (grown on a chip) can be regenerated and utilised for the next binding cycle allowing users to re-probe new interactions on the same receptor sets expressed on the same chip. Evaluation of regeneration conditions is another important step in the cell based binding experiments.

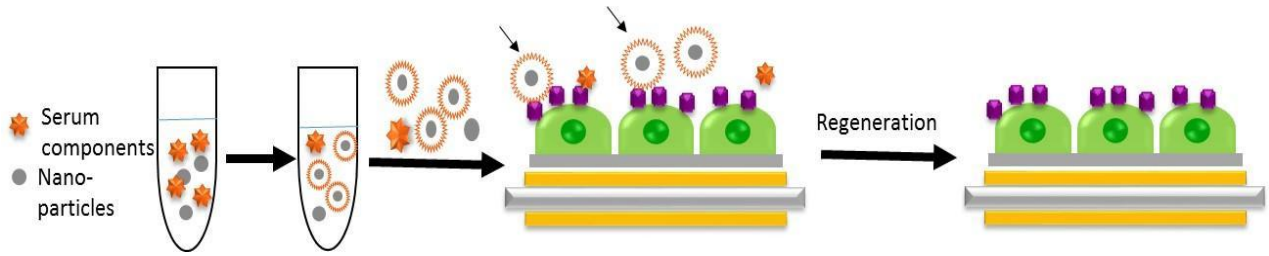

Figure 7: Graphical representation of protein corona formation when MNM incubated with FCS are binding to receptors on cells grown or captured on a sensor chip. Injection of the regeneration solution re-exposes the receptors on the cell surface.

For the purposes of D5.3, fixed cells were utilised (see Section 2.3) as this allows evaluation of the range and sensitivity to the various parameters listed above. However, use of live cells is possible, although the duration of the experiments is a limiting factor as the chamber is not adapted for 5% CO_2 conditions for optimal cell growth. (Note that such an adaption is under development).

2.1 Modification of the hardware component

The Attana system has been developed and designed to perform analysis of crude samples such as sera. However, the combination of sera and MNMs showed a tendency for clogging under extensive use, as a result of agglomeration of the MNM in the serum conditions. Given the scope of Task 5.3, which is delivering a concept for high throughput characterization of MNM-corona interactions with cellular receptors, suitable for use by non-experts, the hardware component of the Attana instrument has been modified to avoid clogging of the equipment during the experiments with MNMs in serum. The standard diameter tubing has been replaced by tubes with larger diameter and necessary modifications of relevant hardware parts have been made with successful results. All experiments reported here were carried out using the prototype equipment which houses larger diameter tubing.

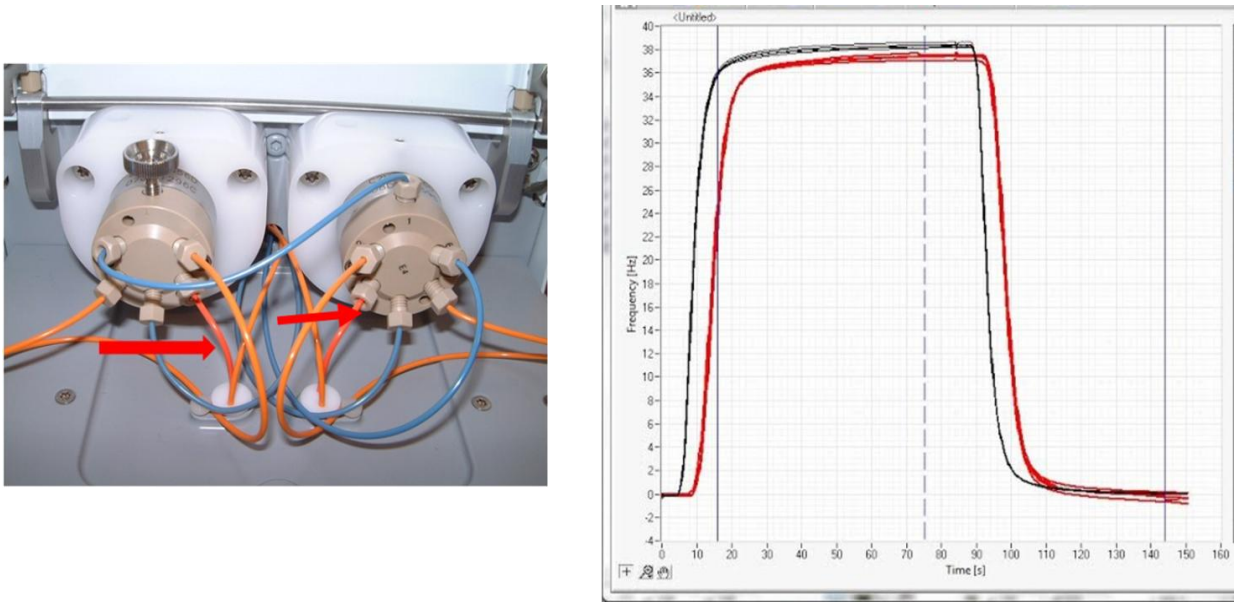

Figure 8: Changes of hardware components and quality control experiment. Left panel: Red arrow shows the larger tubing from the valve to the sensor. Right panel: Comparison of response for 1% DMSO injections for standard tubes (black) and the larger tubes (red). Standard DMSO quality control experiment showed no significant difference of response between the two tubes after necessary component optimizations has been performed.

2.2 Selection of cell lines

Adenocarcinoma human alveolar basal epithelial cells (A549) and adenocarcinoma human colon cell line (Caco-2) were selected as the model cell lines for the development of a cell based QCM platform to study MNMs binding to the cell surfaces. A549 cells were selected to model the cell exposure to MNMs after inhalation and Caco-2 cells were selected to represent cell exposure via ingestion. The A549 cell line is widely used for toxicity studies for lung exposure scenarios. Selection of the cell lines is in agreement with other WP4 and WP5 partners, to ensure alignment of the data generated here with the broader project outputs.

2.3 Fixation of cells using formaldehyde

In the present study cells were grown on the sensor surface and subsequently fixed using 3.7% formaldehyde for 15 min at 25^{o}C. The fixation process enabled regeneration of the cell surface (chemically breaking analyte-ligand interaction) and prevented cellular growth and deterioration. Although formaldehyde fixation process might render some epitopes less accessible this is not considered to alter the overall binding pattern of molecules to cell surfaces (Brooks et al, 1998). Furthermore, fixation of cells with formaldehyde does not necessarily disrupt lateral diffusion of membrane molecules and thus their antibody induced clustering (Tanaka et al, 2010). Mobility of transmembrane proteins, including transferrin receptor, could not be reduced by fixation of cells with 4% formaldehyde for 30 minutes at 25 ^{o}C (Tanaka et al, 2010).

2.4 Seeding density

To examine how seeding density affects the binding capacity of titanium MNMs, COP-1 chips were incubated in cell suspensions with different concentrations corresponding to seeding densities of 2 × 10^4, 4 × 10^4 and 8 × 10^4 cells per sensor surface (15.9 mm^2). After incubation (20 h), cells were fixed with 3.7% formaldehyde, stained with TO-PRO-3 nuclear staining and examined under a fluorescence microscope (Figure 9, A). All chips were shown by fluorescence microscope imaging to exhibit a well distributed monolayer of cell growth, except those seeded with 80,000 cells which exhibited multi-layered formation, indicating that this concentration is too high to be useful for reproducible experimental work.

Next, the binding capacity of the surfaces was examined using titanium dioxide (TiO_2) MNMs: Foetal Calf serum (FCS) injections, varying the ratio of FCS to MNMs. Experiments were performed using Attana cell 200 biosensor (Attana AB) at a flow rate of 20 µl /min at 22 ^{o}C. Binding of TiO2 MNMs (PROM-TiO_2 un-coated) was studied by sequential injections (105 seconds) of the MNM solutions followed by dissociation up to 300 seconds. The maximum frequency response increased with increasing seeding density for all TiO_2 MNM concentrations. Note that the correlation between analyte concentration and the response is normally sigmoidal. However in this situation, a linear increase is observed for both seeding densities 40,000; R^2 =0.99, 20,00 R_2=0.97. A cell seeding density of 4 × 10^4 cells/chip was selected for the successive experiments due to the increased sensitivity.

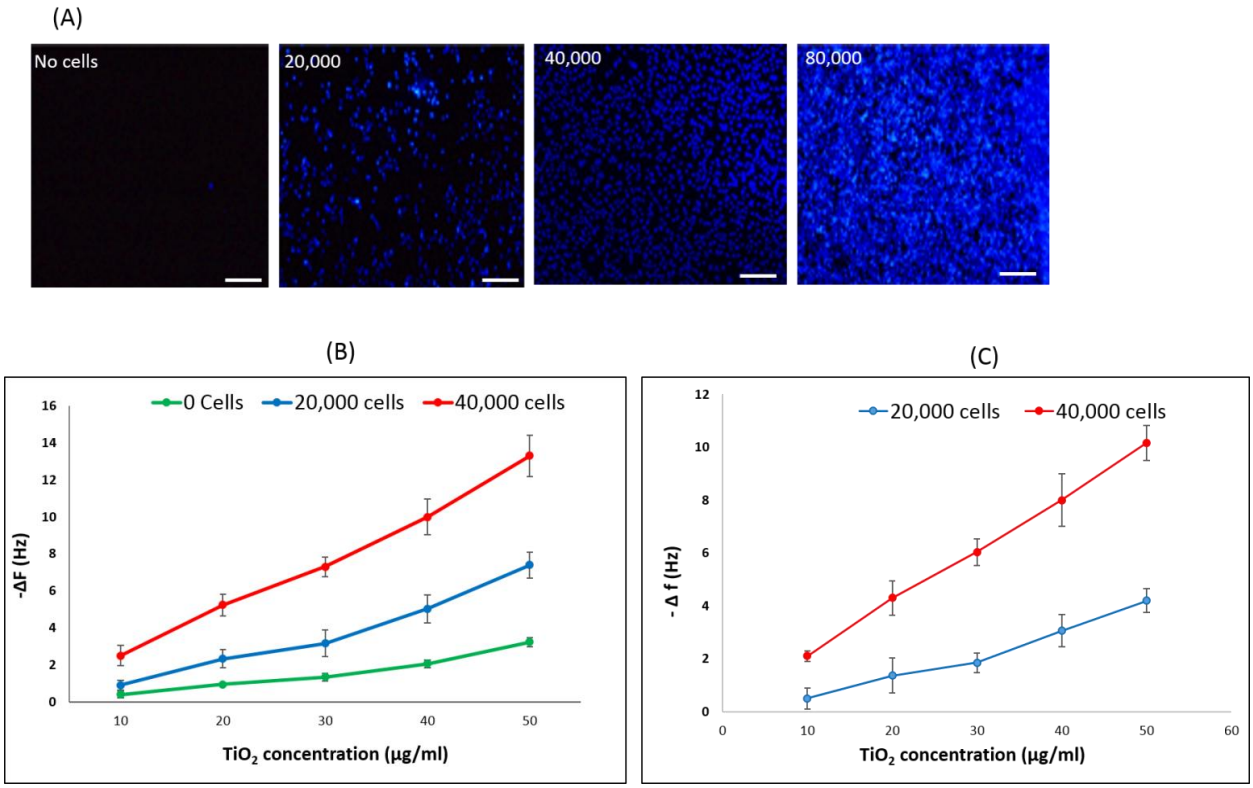

Figure 9: Effect of seeding density on MNM binding. (A) Fluorescence micrographs of To-Pro3 (1mM) stained A549 cells on QCM sensor surfaces prepared using increasing seeding density. Scale bars 200 µm. (B) Maximum frequency response of TiO_2 (PROM-TiO_2 un-coated) MNMs as a function of cell seeding density. (C) Maximum frequency response values normalised to the frequency changes observed for the control sensor surface (no cells). Error bars represent standard deviation (SD) for triplicate injections on three different sensor chips with corresponding seeding density (n=9).

The mass of MNM injected over 105 seconds was calculated for each concentration used and the mass of MNM bound to cells for corresponding seeding concentration was calculated (Table 1). The mass of bound MNMs compared to MNMs flown over is less than 1% for all concentrations, indicating that binding of MNM to the cell surface was not limited by the availability of the MNMs.

Table 1: Determination of the mass of bound MNMs per MNM solution concentration and per cell seeding density. By determining the number of cells/cm^2 of the sensor, it is possible to determine the mass of MNM/cell (average).

Concentration of MNM (µg/ml)	Mass of the particles cells exposed (ng) for 105 sec at 20 µl/min	20,000 cells		40,000 cells	
		Frequency change (Hz)	Mass change (ng)	Frequency change (Hz)	Mass change (ng)
10	350	0.50	0.71	2.10	3.00
20	700	1.37	1.95	4.30	6.14
30	1050	1.85	2.64	6.03	8.61
40	1400	3.06	4.37	8.00	11.43
50	1750	4.20	6.00	10.16	14.51

2.5 Regeneration scouting

In order to remove the bound MNMs and re-expose the cell surface for further experiments, the correct conditions should be used. The regeneration solution should completely remove the bound analyte without disturbing the cell surface receptors. Several regeneration solutions were investigated as part of the optimisation process including:

10 mM- 20 mM Glycine pH1.5-2.5

10 mM HCl

10 mM NaOH pH 8.5.

Two 30 second injections of acidic (10 mM glycine, pH 2) or basic (10 mM NaOH pH 8.5) conditions alone failed to result in a complete regeneration of the cell surface (Figure 10 A and 10 B), however a sequential injection of 10 mM Glycine pH 2 and 10 mM NaOH pH 9.5 resulted in a complete regeneration of the cell surface (Figure 10 C). As the buffer used could potentially lead to irreversible damage to the cell surface epitopes, an analyte, with the same concentration as in the initial experiment, was injected to the cells after complete regeneration to evaluate changes in the binding rate. The cycle of injection and chip regeneration was repeated three times and quite

remarkably no changes in responses was observed, indicating that the cellular surfaces where not affected by the cleaning and regeneration cycle.

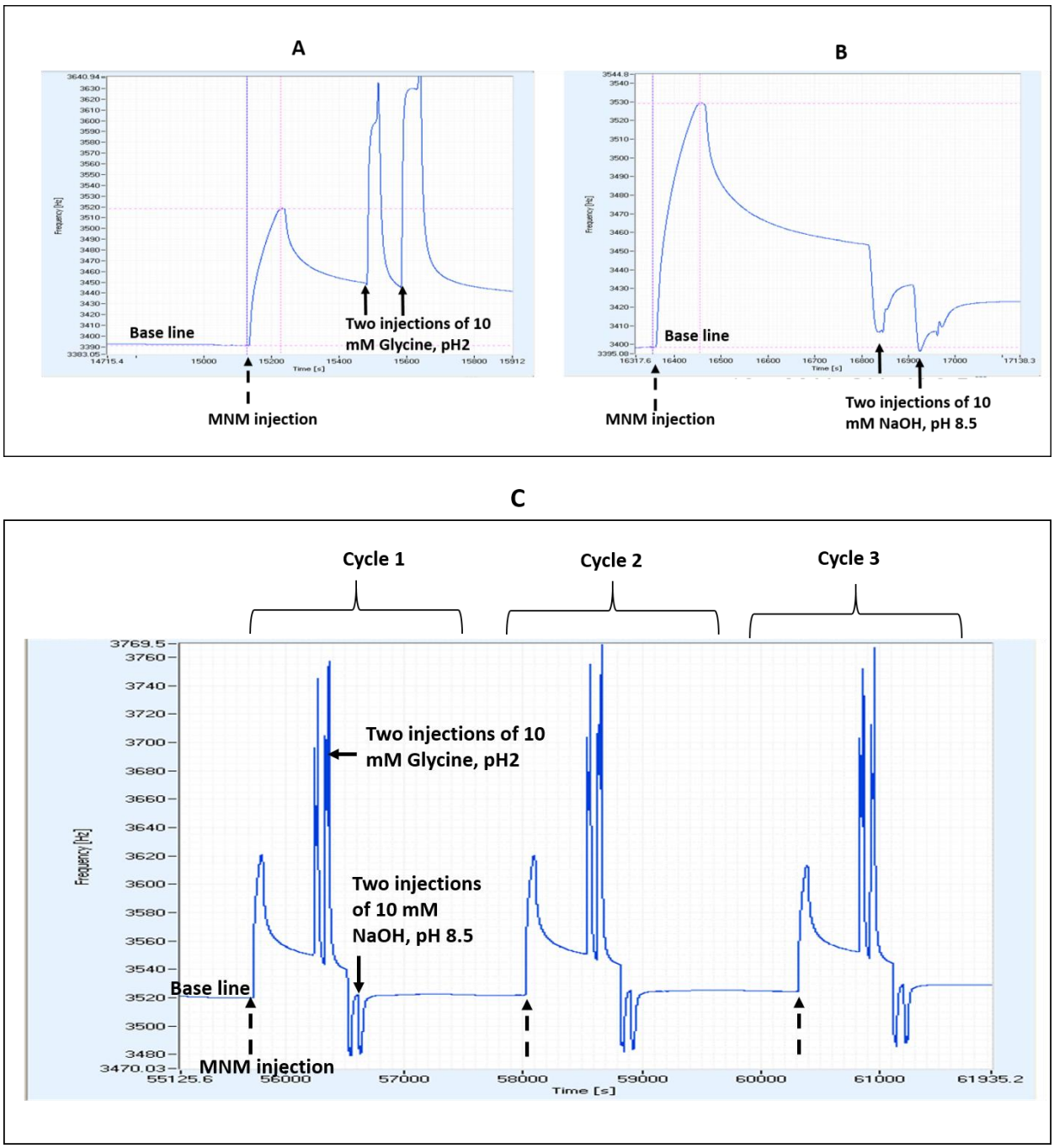

Figure 10: Evaluation of regeneration conditions for the removal of bound FCS:MNMs from the cellular surface. Incomplete/partial regeneration of surfaces exposed to MNMs:FCS by 10 mM glycine (A) or 10 mM NaOH (B). Two sequential injections (30 sec each) of 10 mM Glycine pH 2 and 10 mM NaOH pH 9.5 resulted in complete regeneration of the surface (C). Identical levels of response were observed for the same concentration of the analyte shows the complete removal of analyte from the cell surface and recovery of intact epitopes during the regeneration of the surface.

2.6 Effect of FCS on MNM binding

Since the behaviour of MNMs in complex biological media is defined by the biomolecules absorbed onto their surfaces, studies on interactions between nanoparticles and cell surfaces must be carried out in a biological fluid. The loss of targeting capabilities of transferrin-functionalised nanoparticles in serum (Salvati *et al*, 2013) reiterates the importance of carrying out cell binding assays in appropriate exposure conditions.

In this study, the TiO_2 MNMs has been dispersed in FCS prior flowing over the A549 cell surface. When TiO_2 MNMs were dispersed in PBS running buffer (without FCS) no binding to A549 cell surfaces was observed (Figure 11). A similar observation was made by Canovi et al, (2012) using SPR technology, where poly(methyl methacrylate) (PMMA) MNMs showed no binding to immobilised receptors (anti-HSA and anti-ApoE antibodies and LRP-1 (low-density lipoprotein receptor-related protein) when dispersed in buffer in contrast to the specific binding observed with MNMs pre-incubated in plasma. Dispersion of MNMs in protein-free PBS very likely will lead to rapid irreversible aggregation. The difference in the binding of MNMs in the presence/absence of FCS could thus be either due to the absence of corona proteins in the PBS dispersed particles, indicating the importance of biomolecules at the bio-nano interface for the recognition of cell surface receptors or a result of aggregation state of the MNMs. If the aggregates are large enough to hinder the binding sterically, this could also prevent the binding. However, this needs to be further investigated.

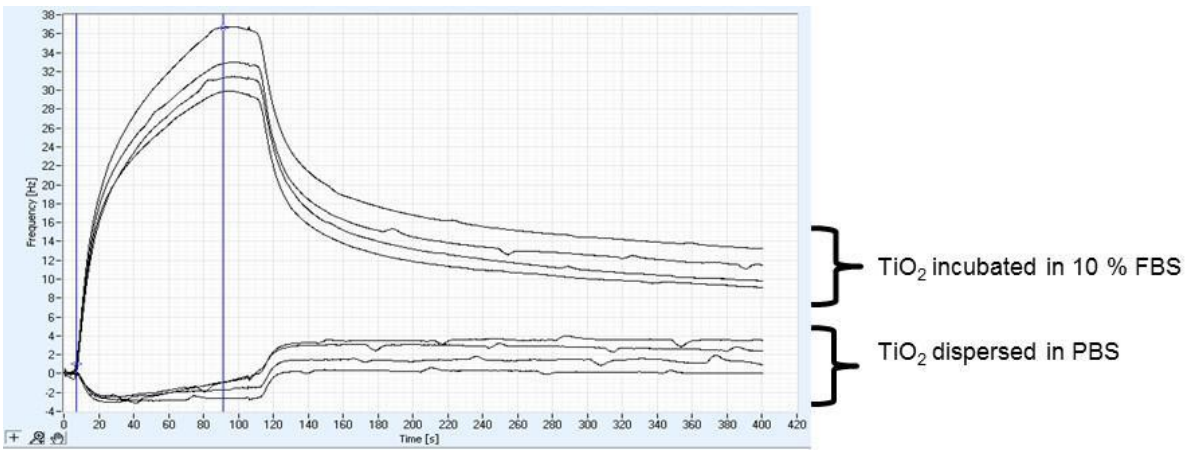

Figure 11: Sensograms showing binding of TiO_2 NMNs dispersed in FCS onto cell surfaces. TiO_2 MNMs dispersed in PBS showed no binding. The initial drop in the case of the PBS-dispersed MNMs is due to the mismatch of solutions: although the MNM were dispersed in PBS (running buffer) they were pre-dispersed in water.

2.7 Effect of particle sedimentation on binding

The binding of a panel of MNMs was then evaluated in the presence of serum. To ensure the highest experimental reproducibility, MNMs that were already dispersed in water (Appendix 1) were bath sonicated for 5 minutes prior to exposure in biological media (10% FCS in PBST, see methods section (Appendix) for additional details).

Samples were loaded into a 96 well plate and injected using an autosampler, however they were mixed immediately prior to the injection with the use of an autosampler syringe. Despite these precautions, duplicate samples prepared using this method did not result in reproducible data as the binding pattern differed significantly. The same observation was made when the duplicate samples were mixed into the media by means of a pipette and manually injected onto the chip (Figure 12 A).

Bath sonication, before and after the first injection, and manual injection resulted in a higher reproducibility of results (Figure 12 B) thus this procedure was used for further experiments. The source of experimental variability has been attributed to MNM sedimentation in biological fluid and thus the experimental validation with a robust and validated protocol is highly important to produce reliable results. Similarly reproducible data were also seen with binding assays of TiO_2 MNMs exposed to Caco-2 cells (Figure 12 C).

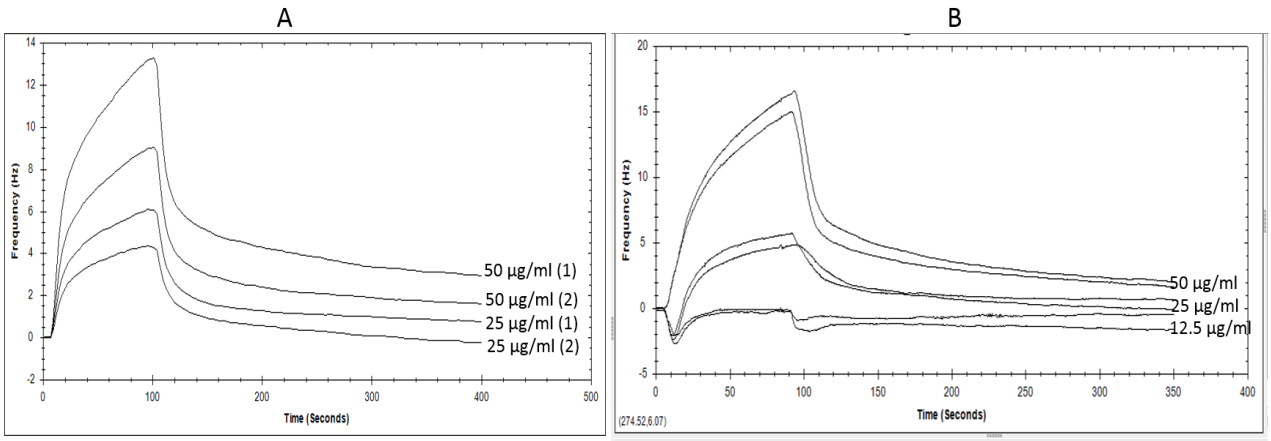

SiO_2-NH_2 particles were mixed using pipette before dispersed in FCS

SiO_2-NH_2 particles were sonicated and dispersed in FCS immediately prior to the injections

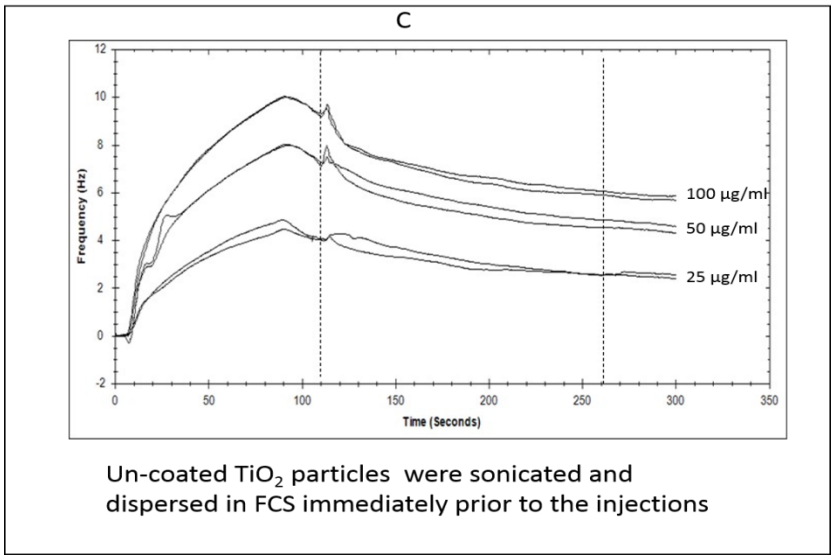

Figure 12: Effect of MNM sedimentation on the reproducibility of the data. Panel A depicts results for injection of 200 µg/mL and 100 µg/mL SiO_2-NH_2 MNMs dispersed in 10% FCS and binding to A549 cells; samples for duplicate injections were prepared at the same time (40 min time lag between duplicate injections). Panel B shows duplicate injections of SiO_2-NH_2 MNM samples (prepared immediately before the injection) at concentrations of 200 µg/mL, 100 µg/mL and 50 µg/mL. (C) concentration dependent binding of uncoated TiO_2 (Promethean particles Ltd) MNMs to A549 cell surface at concentrations of 100 µg/mL, 50 µg/mL and 25µg/mL according to the protocol used in (B).

3.0 METHOD VALIDATION

3.1 Phase I and phase II MNMs screening

TiO_2, Ag, CeO_2, printex 90 and SiO_2-NH_2 and SiO_2-COOH MNMs were selected for the screening for binding to A549 and Caco-2 cell lines and the findings are shown in Table 2**.** With the exception of the citrate modified Ag particles, none of the other MNMs tested showed binding to the surfaces of either of the cell lines in the absence of serum. Very low binding of Ag-citrate particles (100 nm and 60 nm) dispersed in PBS was observed when exposed to the A549 cell line. In the presence of serum, TiO_2 and SiO_2-NH_2 and SiO_2-COOH MNMs bind to both A549 and Caco-2cell lines. Hence the corona mediates binding of certain MNMs and surface functionalisation has a clear impact on binding, presumably due to increased adsorption of proteins (Figure A1 in the Appendix shows the differences in protein adsorption patterns with different MNMs incubated in NanoMILE FCS).

Table 2: Screening of TiO_2, Ag, CeO_2, printex 90 and SiO_2-NH_2 and SiO_2-COOH MNMs dispersed in FCS for binding to A549 and Caco-2 cells grown on sensor chip surfaces.

	A549 cells	Caco2 cells
TiO_2 (Prom – un)	Binds when dispersed in 10% FCS	Binds when dispersed in 10% FCS
TiO2 (Prom) PVP coated	Binds when dispersed in 10% FCS	Binds when dispersed in 10% FCS
Ag (JRC)	No binding	No binding
Ag-cit (Sigma)	Binds when dispersed in 10% FCS or dispersed in PBS Low response.	Binds when dispersed in 10% FCS
CeO_2 (JRC-uncoated)	No binding	No binding
Printex 90 (NRCWE)	No binding	No binding
SiO_2(JRC)	No binding	No binding
SiO_2-COOH (JRC)	Binds when dispersed in 10% FCS	Binds when dispersed in 10% FCS
SiO_2-NH_2 (JRC)	Binds when dispersed in 10% FCS	Binds when dispersed in 10% FCS

3.2 Monitoring of SiO_2 particles binding to the surface of A549 cells

Unmodified SiO_2 MNMs dispersed in FCS did not bind to either A549 or Caco-2 cell surfaces, however SiO_2 particles conjugated with primary amine groups (SiO_2-NH_2) and carboxyl groups (SiO_2-COOH) did (Figure 13). As the protein corona composition is known to be correlated with the MNM surface properties, future studies will attempt to elucidate differences in the protein corona composition on these MNM and from this provide some explanation about the difference in binding to cells.

Figure 13B shows the off rate data (k_d), which corresponds to the rate / amount of the initially adsorbed MNMs that dissociate from the chip during the flowing of buffer for 300 s, derived from the sensorgrams corresponding to the various silica MNMss. The two k_d values were determined using TraceDrawer software (Ridgeview AB, Sweden), which uses the Levenberg–Marquardt algorithm for curve-fitting. There were no notable differences between the off rates of different sizes of SiO_2-NH_2 or SiO_2-COOH MNMs in terms of MNM mass, and this could also be calculated as the rate of MNMs detaching, suggesting that for the same mass change there are 15.6 times more MNMs detaching when considering 20nm MNMs compared to 50nm MNMs. For the specific

binding component, the off rate constants (k_{d2}) range from 1.99 E^{-3} to 3.79 E^{-3}. This indicates that binding strengths to the polystyrene coated sensor surface are similar for SiO_2-NH_2 or SiO_2-COOH MNMs, although it doesn't necessarily imply similar binding events or involvement of similar receptors. Additional studies, for example using competitive conditions with proteins known to bind to specific receptors, would be needed to elucidate which specific receptors are involved in binding of the different MNMs.

A

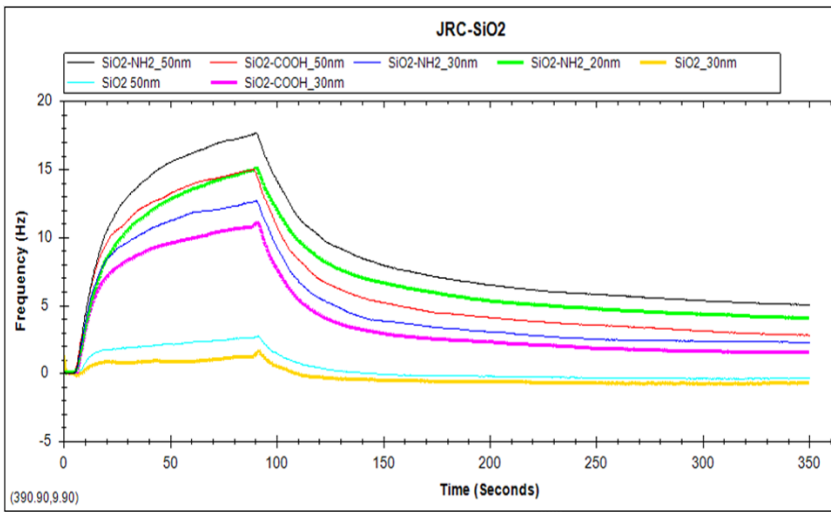

B

Particle	kd1	kd2
SiO2-NH2 (20nm)	4.12E-3	1.99E-3
SiO2-NH2 (30nm)	5.52E-3	2.79E-3
SiO2-NH2 (50nm)	4.36E-3	2.14E-3
SiO2-COOH (30 nm)	7.23E-3	3.79E-3
SiO2-COOH (50nm)	6.18E-3	3.12E-3

Figure 13: Effect of surface modifications of MNMs on binding to the Attana COP-1 chip. (A) Sensorgram for SiO_2 MNMs of different size and surface functionalisation (JRC) binding to A549 cell surface. Amine or carboxyl modified SiO_2 particles showed binding to A549 cell surface at a flow rate of 20 µL/min. SiO_2 NPs without surface modification, showed no binding under the same conditions. (B) Off rates of SiO_2MNM dissociation at two time points, corresponding to target and off-target binding determined using the Levenberg–Marquardt algorithm.

This observation is in agreement with the immunofluorescence data (shown in Figure 14) where $Ru(Bpy)_3$ conjugated SiO_2 particles were employed to study the binding of SiO_2 MNMs to A549 cells using confocal microscopy.

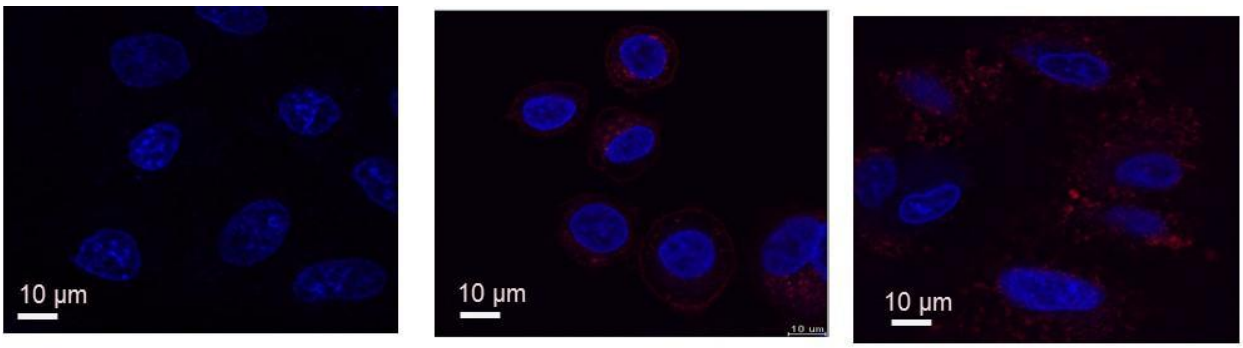

SiO_2 Ru(Bpy)3 SiO_2-NH_2-Ru(Bpy)3 SiO_2- COOH Ru(Bpy)3

Figure 14: Confocal images showing $Ru(BPy)_3$ labelled SiO_2 MNMs binding to A549 cells. Cells were incubated with $Ru(BPy)_3$ labelled SiO_2 MNMs and counter stained with 1 mM To-Pro3.

3.3 Monitoring of TiO_2 particles binding to A549 cell surface

After the initial screening of the Phase I MNMs, a panel of TiO_2 particles with a range of different surface coatings were selected (see Table 3) and monitored for binding to the A549 cell surface.

MNM	Size	Source
NIST TiO_2	~ 70 nm primary particle	NIST
TiO_2 - Uncoated	10 nm primary particles	PROM
TiO_2 - PVP coated	10 nm primary particles	PROM
TiO_2 - Pluronic F127 coated	10 nm primary particles	PROM
TiO_2 - Dispex AA4040 coated	10nm primary particles	PROM
TiO_2 NM103 - hydrophobic	20 nm primary particles	PROM
TiO_2 NM104 - hydrophilic	20 nm primary particles	PROM

Table 3: TiO_2 MNMs selected for the binding experiments with A549 cells grown on sensor chip surfaces. Particle size of NIST TiO_2 was determined using DLS in water and the particle size of other MNMs were determined using TEM. NIST- National Institute of Standard Technology, PROM- Promethean Particles Ltd.

Interestingly, un-coated, PVP coated and NM104 TiO_2 MNMs dispersed in 10% FCS showed binding to A549 cell surfaces, with the sensorgrams and off rate values for specific and un-specific binding given in Figure 15 below, while TiO_2 (NIST), TiO_2 MNMs coated with Pluronic F127, Dispex AA4040 and hydrophobic NM103 MNMs did not show any interaction with the same cell type.

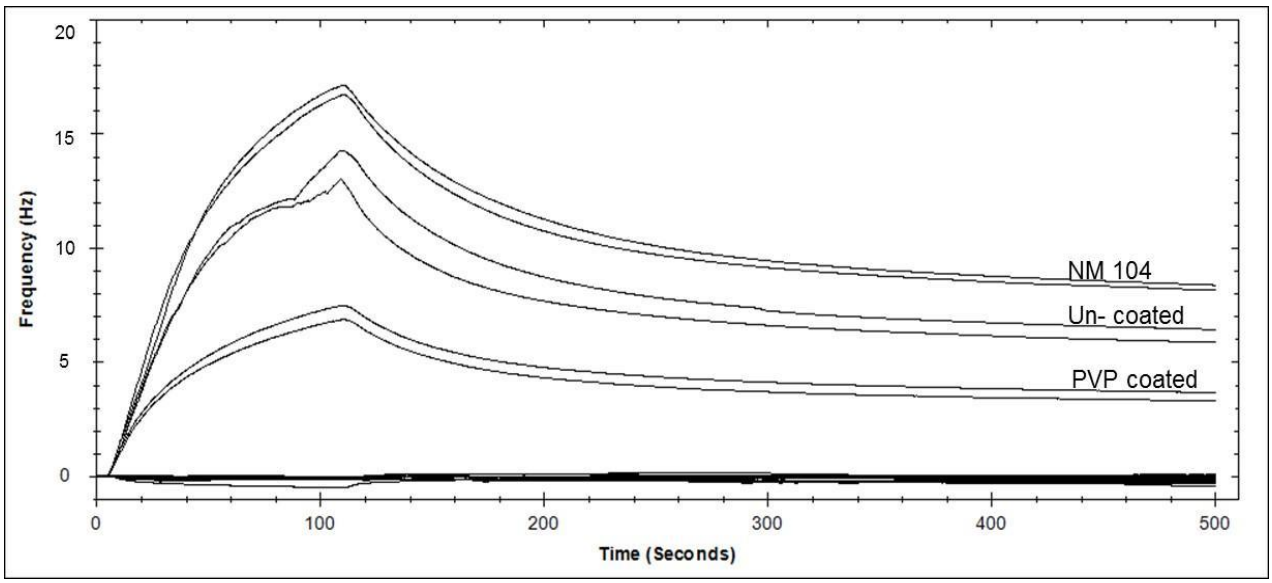

Particle	kd1	kd2
Surface-modified TiO_2 -surface 1 (Uncoated)	6.3 E-3	4.98 E-4
Surface-modified TiO_2- surface 1 (PVP coated)	5.7 E-3	5.31 E-4
Titanium Dioxide (rutile, hydrophilic) NM-104	5.1 E-3	5.03 E-4

Figure 15: Effect of surface modification (coating/capping) of MNM on binding to A549 cells. (A) Sensograms for TiO_2 MNMs binding to the surface of A549 cells. Un-coated, PVP coated and rutile hydrophilic (NM104) TiO_2 MNMs showed binding to the cell surface, while TiO_2 (NIST), Pluronic F127 coated, Dispex AA4040 coated and NM103 MNMs show no binding. (B) Off rates of TiO_2 MNMs dissociation at two time points, corresponding to target and off-target binding, respectively, determined using the Levenberg–Marquardt algorithm.

3.4 Individual plasma protein coated MNMs and their interactions with the surface of A549 cells.

It is believed that the MNM corona is primarily formed by the 20 most abundant proteins (in serum), however the overall protein composition can be composed of several hundreds of proteins (Monopoli et al 2012; Tenzer et al 2013). In order to profile specific interactions, in this experiment we have allowed the formation of a protein corona with selected single proteins (rather than full serum) prior to exposure to the cell surface, with preliminary studies performed using bovine serum albumin (BSA), bovine transferrin and fibrinogen. Quite interestingly TiO_2-uncoated (Promethean particles Ltd) MNMs incubated with BSA did not show binding to the A549 cell surface, however when the same MNMs were incubated with transferrin, an interaction with the cellular surface was detected (Figure 16). Fibrinogen coated TiO_2 MNMs showed a very low binding response compared to transferrin-coated TiO_2 MNMs.

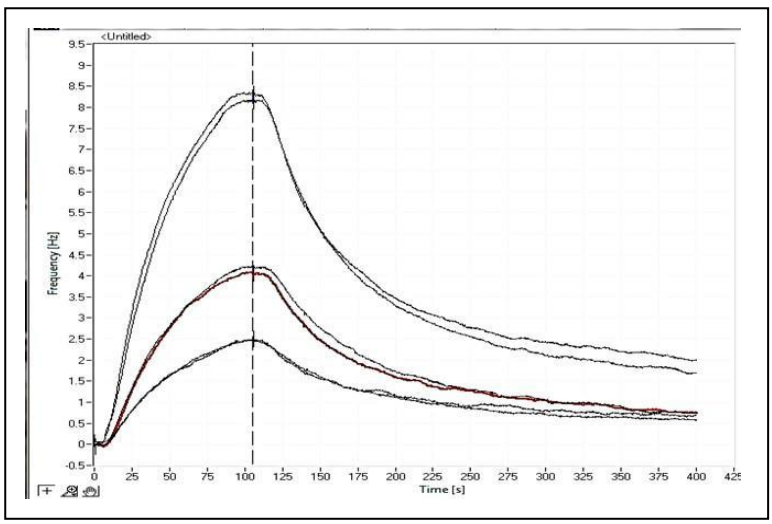

kd1 – 3.5 E^{-3}

kd2 – 1.9 E^{-4}

Figure 16: Transferrin coated TiO_2 MNM binding to A549 cell surface. TiO_2 MNMs (200 µg/mL) were incubated in 1 mg/mL of transferrin solution and centrifuged to separate the protein coated MNMs, washed three times in PBS and flown over A549 cells grown on sensor surface.

The hard corona proteins bound toTiO_2 MNMs and SiO_2 MNMs incubated with FCS were analysed using SDS-PAGE (see Figure A1 in the Appendix). SDS- PAGE analysis showed a complex mixture of proteins bound to the MNMs, including albumin. This indicates that the differences in binding of individual protein coated MNMs might not be due to the absence of particular protein in the corona, but rather, due to the differences in the binding affinities of the corona-coated MNMs to the cell surface receptors. For instance, albumin or fibrinogen coating the MNMs alone did not facilitate binding of the MNMs to the A549 cell surface. However, interaction studies of metal oxide MNMs (SiO_2, TiO_2 and ZnO) incubated with fibrinogen showed positive binding to the integrin receptor, MAC-1 positive cell line, THP-1 (Deng et al, 2010). The absence of binding of fibrinogen incubated TiO_2 MNMs to A549 cells might be due the absence or low expression of relevant receptors including MAC-1 on A549 cells. However, this need to be investigated further with different cell lines including MAC-1 positive cells.

4.0 Conclusions and future work

A QCM based methodology has been developed for the screening of MNMs including in the presence of complex biological fluids for assessment of MNM and MNM-corona interactions with cell surfaces. Task 5.3 has successfully demonstrated that the Attana label free cell based system can be utilised to study MNM-protein-cell interactions. This system allows the study of binding interactions in the presence of other biomolecules that are found at the cell surface in contrast with a conventional experimental set up using planar systems where single protein entities are investigated. The hardware features of the Attana system allow performance of experiments using biological fluids such as serum. Furthermore, interactions can be monitored under continuous flow, which mimics the circulation of MNMs in the body. The real time, label free approach presented here may facilitate the understanding of mechanisms involved in MNM binding to cell surfaces, in particular identifying the binding partners at the bio-nano interface. Future studies will be mainly concerned with identifying the binding partners and relating them to specific features of the MNM biomolecule corona and the underlying MNM surface and core chemistries. The approach used in the final section, namely investigation of individual serum components, will be used in order to identify selective binding of proteins to MNMs and biological receptors at cellular surfaces.

In its current state, the instrumental setup of the Attana cell 200 allows analysis of 192 samples unattended using an automated c-fast system. During the automated analysis, samples need to be placed into the instrument prior to experiments, and the time lag between the injections of samples can be up to 30-40 min. However, the methodology developed here for the analysis of MNM in FCS requires manual injections, because samples need to be prepared immediately prior to injection to avoid sedimentation of the MNMs. Automated injections of MNMs can be achieved if the samples can be sonicated in the instrument with the use of an integrated sonicator. Attana will continue to pursue this by introducing new hardware/software components and are willing to collaborate with other NanoMILE partners on this aspect. Success of this new development will significantly increase the throughput of the sample analysis.

In addition, the effect of sedimentation of MNMs on the reproducibility of binding events will be further investigated. Differential Centrifugal Sedimentation (DCS) analysis of FCS dispersed MNMs will be carried out in detail to understand the effect of prolonged exposure to biological fluids on sedimentation and the subsequent MNM binding to cellular receptors.

References

Brooks, S.A., Dwek, M.V., Leathem, A.J.C. Release and analysis of polypeptide and glycopeptides from formalin-fixed paraffin wax embedded tissue. Histochemical Journal 1998, 30: 609-615.

Canovi, M., Jacopo Lucchetti, J., Matteo Stravalaci, M., Re, F., Moscatelli, D., Bigini, P., Salmona, M. and Gobbi, M., Applications of Surface Plasmon Resonance (SPR) for the Characterization of Nanoparticles Developed for Biomedical Purposes. Sensors 2012, 12, 16420-16432.

Deng, Z.J., Liang, M., Monteiro, M., Toth, I., Minchin, R.F. Nanoparticle-induced unfolding of fibrinogen promotes Mac-1 receptor activation and inflammation. Nature Nanotechnology 2010. 6: 39-44.

Elmlund, L., Kack, C., Aastrup T. and Nicholla, A. Study of the interaction of Trastuzumab and SKOV3 epithelial cancer cells using a quartz crystal microblance sensor. Sensors 2015, 15: 5884-5894.

Goppert, T.M., Muller, R.H. Adsorption kinetics of plasma proteins on solid lipid nanoparticles for drug targeting. Int. J Pharm. 2005; 302:172–186.

Li, X., Pei, Y., Zhang, R., Shuai, Q., Wang, F., Aastrup, T., Pei, Z. A suspension-cell biosensor for real-time determination of binding kinetics of protein–carbohydrate interactions on cancer cell surfaces. Chem.Commun., 2013. 49: 9908.

Li, X., Song, S., Shuai, Q., Yihan Pei, Y., Aastrup, T., Pei, Y., Pei, Z. Real-time and label-free analysis of binding thermodynamics of carbohydrate-protein interactions on unfixed cancer cell surfaces using a QCM biosensor. Scientific Reports, 2015. 5, Article number: 14066. doi:10.1038/srep14066

Lundqvist, M., Stigler, J., Cedervall, T., Berggard, T., Flanagan, M.B., Lynch, I., Elia, G., Dawson K. The evolution of the protein corona around nanoparticles: a test study. ACS Nano 2011; 5:7503–7509.

Monopoli, M.P., Åberg, C., Anna Salvati, A., Dawson, K.A. Biomolecular coronas provide the biological identity of nanosized materials. Nature Nanotechnology. 2012; 7; 779-786

Monopoli, M.P., Walczyk, D., Campbell, A., Elia, G., Lynch, I., Baldelli B., Dawson, K.A. Physical-chemical aspects of protein corona: relevance to *in vitro* and *in vivo* biological impacts of nanoparticles. Journal of American Chemical Society. 2011; 133:2525-2534.

Nel, A.E., Madler, L., Velego, D., Xia, T., Hoek, E.M.V., Somasundaran, P., Klaessig, F., Castranova, V., Thompson, M. Understanding bio-physicochemical interactions at the nano–biointerface. Nature Material. 2009; 8: 543–557.

Peiris, D., Markiv, A., Curley, G. P., Dwek, M. V. A novel approach to determining the affinity of protein–carbohydrate interactions employing adherent cancer cells grown on a biosensor surface. Biosensors and Bioelectronics. 2012; 35:160– 166

Rahman, M., Laurent, S., Tawil, N., Yahia, L., Mahmoudi, M., Protein-Nanoparticle Interactions, Springer Series in Biophysics 15, Springer-Verlag Berlin Heidelberg 2013

Sakulkhu, U., Maurizi, L., Mahmoudi, M., Motazacker M., Vries, M., Gramoun, A., Beuzelin, M.O., Vallee, J., Rezaee, F., Hofmann, H. Ex situ evaluation of the composition of protein corona of intravenously injected superparamagnetic nanoparticles in rats. Nanoscale. 2014; 6:11439-11450

Salvati, A., Pitek, A.S., Monopoli,M.P., Prapainop,K. Bombelli,F.B., Hristov,D.R., Kelly,P.M., Åberg, C., Eugene Mahon, E., Kenneth A. Dawson, K.A. Transferrin-functionalized nanoparticles lose their targeting capabilities when a biomolecule corona adsorbs on the surface. Nature Nanotechnology letters 2013, 8: 137-143.

Tanaka, K.A., Suzuki, K.G., Shiraj, Y.M., Shibutani, S.T., Miyahara, M.S. Tsuboi, H., Yahara, M., Yoshimura, A., Mayor, S., Fujiwara, T.K., Kusumi, A. Membrane molecules mobile even after chemical fixation. Nature methods 2010. 7: 865-866.

Tenzer, S., Docter, D., Kuharev, J., Musyanovych, A., Fetz,V.,Hecht, R.,Schlenk, F., Fischer, D., Kiouptsi,K., Reinhardt,C., Landfester, K., Schild, H., Maskos, M., Knauer S.K., Roland H. Stauber, R.H. Rapid formation of plasma protein corona critically affects nanoparticle pathophysiology. Nature Nanotechnology. 2013; 8:773-781

Walczyk, D., Bombelli, F.B., Monopoli, M.P., Lynch,I., KA Dawson, K.A. What the cells "sees" in bionanoscience. Journal of the American Chemical Society. 2010 132:5761-5768.

Yazdan Madani, S., Tan, A., Dwek, M., Seifalian, A.M. Functionalization of single-walled carbon nanotubes and their binding to cancer cells. Int J Nanomedicine. 2012; 7: 905–914.

Appendix – Supporting data and protocols

SDS page analysis of hard corona proteins

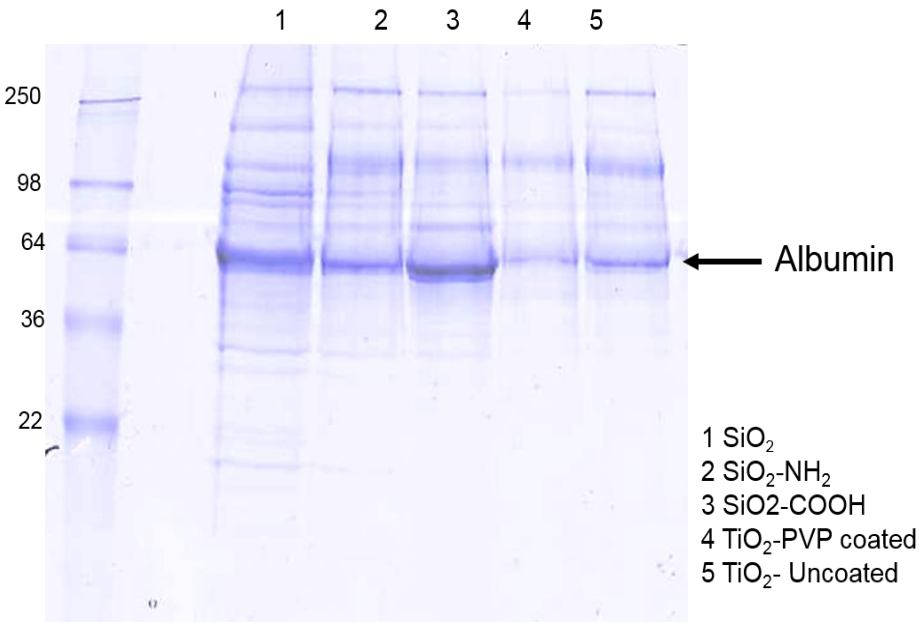

Figure A1: SDS-PAGE of isolated corona proteins associated with SiO_2 and TiO_2 MNMs incubated in .

One dimentional sodium dodecyl sulfate-polyacrylamide gel electrophoresis was performed on the proteins isolated after incubation of MNM for 1 hr. Removal of the hard corona was achieved by sonicating nanoparticles in Laemmli buffer (63 mM Tris-HCl, pH 6.8, 40 mM DTT, 0.01% (w/v) bromophenol blue, 10% glycerol , 2% (w/v) SDS. Particle was boiled for 5-10 min at 95 ^{O}C and the supernatant was collected after centrifugation at 14,000 rpm for 5 min. Gel electrophoresis was performed at 120 V for 1.5 hrs and gel was stained with coomssie blue.

Methods

Protocol used for the dispersion of materials TiO_2 (NM103 and NM104) or CeO_2 (NM212) from the JRC repository.

This dispersion protocol has been verified for the preparation of MNM dispersions at a concentration of 10mg/ml.

The dispersion protocols which have been used for the repository MNMs have been implemented using probe sonication. It is preferable that the sample be placed in an ice-bath when using a probe sonicator.

1) Weight 50-100 mg of NM into an appropriate centrifuge tube.
2) Add high purity water to make a 10 mg/ml solution (solution A). Vortex 2-3 min.
3) If using a probe sonicator, the dispersion should be verified using DCS or DLS measurements of sample sonicated for 1, 5, 10 and 15min to establish the minimum treatment time beyond which no further reduction in mean particle size is observed. The ultrasonic energy should have an amplitude of 75% and cycle time 0.5. For the samples used in this report, the following optimal sonication times were obtained:
   - TiO_2 NM103: 10min
   - TiO_2 NM104: 1min
   - CeO_2 NM 212: 5min
   - CeO_2 NM 211: 1min
   - TiO_2 NIST: 5min
4) If samples are not used immediately following dispersion the quality of dispersion achieved with the probe sonicator can be regained by treating the sample to 5 minutes of sonication in a normal bath sonicator. This has been verified by JRC for sample stored for more than 4 weeks (needs to be checked by UoB).

Production of sterile-filtered BSA water:

The production of 0.05% w/v BSA-water (the dispersion medium) is done in two steps: 1) Preparing a sterile-filtered 1% w/v BSA stock solution, and 2) Dilution to reach a 0.05% w/v BSA dispersion medium.

a. Procedure for making a 1% w/v BSA water stock solution:

1) Add from pipette 50 ml Nanopure (or MilliQ) water to a 100 ml mixing flask (e.g., re-useable acid-washed blue-cap flasks or similar).
2) Weigh out 1 g BSA (powder) in a weighing boat and pour it into the flask with 50 ml water, rinse the weighing boat into the mixing bottle with Nanopure (or MilliQ) water to retrieve as much BSA as possible into the mixing flask.

3) Fill the mixing flask up until 100 ml using Nanopure (or MilliQ) water to reach a 1 % w/v BSA-water solution.

4) Gently stir or swirl the BSA-solution for a few minutes (be careful to avoid foam by not using agitated stirring) and leave the mixing flask in the refrigerator over-night for complete dissolution of the BSA.

5) Sterile filter the 1% w/v BSA-water solution into a new flask through an 0.2 µm sterile disposable filter after complete dissolution of BSA in the mixing flask. It was found that this sterile filtration causes about 28% loss of BSA and hence, the true BSA concentration in the final so-called 0.05% w/v BSA solution is in fact of 0.036% w/v as determined by a Pierce BCA protein Assay Kit for microplate reading. However, we have kept the 0.05% notation in accordance with the direct dilution procedure below.

b. Procedure for making the "0.05% w/v BSA-water solution" for nanomaterial dispersion:

The 0.05% w/v BSA solution to be used for test item preparation is achieved by simple dilution of the sterile-filtered 1% w/v BSA batch solution. Remember that the 0.05% w/v BSA solution in reality contains ca. 0.036% BSA w/v due to loss in the sterile-filtration.

Example: 2 ml 1 % w/v BSA is diluted with 38 ml Nanopure water (or MilliQ) (Dilution factor = 20x) to reach a batch solution of "0.05% w/v."

Calculations for preparing the 2.56 mg/ml EtOH-prewetted stock dispersion

For preparing a 2.56 mg/mL stock dispersion in a 6 ml EtOH-BSA-water, each vial must contain at least 15.36 mg MNM. For harmonization of the dispersion energy it is recommended to stay as close as possible to a total volume of 6 ml EtOH + BSA-water.

Calculation of the correct volume is according to equation 1:

1: $V = m / c$

m = mass of MNM (mg)

c = concentration (normally 2.56 mg/mL)

V = volume of dispersion medium (mL)

6 ml is required to disperse 15.36 mg powder at the target concentration of 2.56 mg/ml.

0.5 vol% EtOH (96% or higher) is used for pre-wetting: 6 mL x 0.5/100 = 0.03 mL (30 µL) EtOH

99.5 vol% sterile-filtered BSA-water (0.05% w/v) is used as dispersion medium: 6 – 0.03 = 5.97 ml BSA-water.

Procedure for MNM dispersion

MNMs are pre-wetted using EtOH. This procedure was introduced to enable dispersion of hydrophobic MNMs in water-based systems, but in this protocol, we have introduced EtOH pre-wetting for all MNMs in order to harmonize the treatment for all powder MNMs.

Pre-wetting procedure (volumes for 15.36 mg powder)

1) Carefully open the glass scintillation vial with pre-weighed powder (ideally 15.36 mg).
2) Tilt the scintillation vial ca. 45° and add 30 µL EtOH drop-by-drop onto the particles in the vial by pipette.
3) Screw on the lid and gently mix the EtOH and powder by simultaneous gently tapping the vial on the table-top while rotating the 45° tilted vial from side to side between your fingers for approximately one minute.
4) Add 970 µL 0.05 % BSA water by pipette while slowly rotating and swirling the 45° tilted scintillation glass. Be careful to avoid foaming of BSA. The last mL or so of BSA-water is added along the top of the inner wall of the vial to collect the powder in the fluid at the vial bottom.
5) Add the remaining 5 mL 0.05 % BSA water by pipette along the sidewalls of the scintillation vial to wash down any particles that may be stuck to the sidewalls.
6) Place the vial on ice for at least 5 minutes while the sonicator and ice-water are prepared.

Sonication procedure

1) Fill a 250 mL glass beaker with ice and place it upside-down in a insulation box (flamingo/styrofoam)
2) Add ca. 85-90 vol% ice into the insulation box
3) Add ca. 10-15 vol% cold water into the insulation box
4) Carefully place the glass scintillation vial with powder on top of the upside-down glass-beaker and pack the ice-water around the vial to keep the dispersion cooled. One may fix

the vial using a clip or burette holder to ensure that the vial does not move during sonication.

5) Insert the sonication probe (between the upper quarter and upper half of the BSA-water volume in the scintillation beaker (e.g., find the correct height using a vial with BSA-water alone).

6) Start sonication and run it for 16 min at 400 W and 10% amplitude while controlling that the sonication probe does not touch the walls of the scintillation vial. Use of different sonication conditions (power and amplitude) may require different sonication times. The energy input should be calibrated to be on the order of 3,136 MJ/m^3.

7) Remove the scintillation vial and add the lid.

8) Clean the sonication probe by sonication for 5 minutes (similar sonication settings) with the probe fully immersed in a 50:50 water-EtOH (>96%) mixture followed by rinsing in EtOH using a dispenser and a collection bottle underneath. The probe is allowed to air-dry in the fume-hood. Other in-house cleaning methods may also apply.

After sonication, the dispersions should be checked for quality and final MNM size and size distribution in dispersion using dynamic light-scattering (DLS) or similar techniques.

Preparation of samples for QCM

- Filter FCS (the NanoMILE centralised serum (Gibco)) using 0.1µm filter.
- TiO_2 and SiO_2 MNMs (already dispersed in deionised water) are sonicated for 5 min in water bath immediately prior to use.
- Disperse MNMs at appropriate final concentration either in PBST (PBS + 0.05% tween) running buffer or 10% FCS.

Preparation of cell–biosensor surface

- A459 or Caco-2 cells were grown in Dulbecco's modified Eagle's medium (DMEM, Lonza, UK) supplemented with 10% (v/v) foetal bovine serum (Biosera).
- Cells were cultured using standard tissue culture techniques. Cells were grown on cell culture compatible polystyrene coated surfaces (COP-1) (Attana AB, Sweden) and incubated at 37 ^{o}C (5% (v/v) CO_2 and 95% humidity for 18-20 hours.

- Following incubation cells were fixed in fresh 3.7% (v/v) formaldehyde in PBS for 20 min. To evaluate the cell coverage the nuclei were stained with 1 mM To-Pro 3 and visualised using a fluorescence microscope.

Introductory studies on cell surface

- Experiments were performed using a modified Attana cell 200 biosensor (Attana AB) at a flow rate of 20 µL /min at 22 ^{o}C. The fluidics of the biosensor have been modified with new tubing optimised for use with MNM and sera in combination.
- Sensor chips were inserted into the machine and running buffer (PBST) was passed over the sensor surface until stabilisation of the baseline (frequency change ≤ 2 Hz over 600 s) was achieved.
- The binding of MNMs was studied by sequential injections (105 seconds) of the MNM solutions followed by dissociation up to 300 seconds. Duplicate injections were performed for each MNM using individually prepared samples.
- After binding and dissociation of MNMs or sera, the surface was regenerated using 30 sec sequential injections of 20mM Glycine, pH 2 and 10 mM NaOH at pH 8.0.
- The frequency changes during binding experiments were recorded using Attestar software (Attana AB) and analysed using Evaluation software (Attana AB). Blank injections of 10% FCS were subtracted from the MNMs: FCS injections.